

# Kallistatin alleviates heart failure in rats by inhibiting myocardial inflammation and apoptosis *via* regulating sirt1

J. XIE<sup>1</sup>, Q.-G. YU<sup>1</sup>, L.-L. YANG<sup>1</sup>, Y.-Y. SUN<sup>2</sup>

<sup>1</sup>Department of General Medicine, <sup>2</sup>Department of Clinical Nutrition; Hefei Hospital Affiliated to Anhui Medical University, The No. 2 People's Hospital of Hefei, Hefei, China

**Abstract.** – **OBJECTIVE:** Heart failure (HF) is the loss of myocardial structure and function caused by various congenital or acquired heart diseases. This study explored the new target of treatment of HF by investigating the effect of Kallistatin (KS) on inflammation and apoptosis of myocardial tissue in HF rats.

**MATERIALS AND METHODS:** We used doxorubicin to induce rat HF, and determined the success rate of modeling by detecting changes in rat heart weight and body weight, cardiac function and histology. We used two different doses (1 mg/kg, 2 mg/kg) of KS intraperitoneally injected rats and detected changes in inflammation and apoptosis of rat myocardial tissue by enzyme-linked immunosorbent assay (ELISA), Reverse Transcription-Polymerase Chain Reaction (RT-PCR) and immunohistochemical staining. Changes in the expression of sirt1 were also detected. In addition, we cultured rat myocardial cell line, H9c2 cells, and used siRNA-sirt1 to inhibit sirt1 in H9c2 cells to clarify the mechanism of KS regulating myocardial cells.

**RESULTS:** The body weight of HF rats treated with KS decreased while the heart weight increased. KS has also been found to reduce the concentration of brain natriuretic polypeptide (BNP) in rat serum. The results of echocardiography showed that KS effectively relieved the cardiac function of HF rats. Inflammatory factors (interleukin (IL)-1 $\beta$ , IL-6, IL-8 and tumor necrosis factor (TNF)- $\alpha$ ) and pro-apoptotic molecules (caspase3/9 and Bax) in the serum and myocardial tissue of rats treated with KS were also significantly reduced. The inhibition of sirt1 in H9c2 cells significantly reduced the anti-apoptotic effect of KS on H9c2 cells.

**CONCLUSIONS:** KS reduces the inflammation and apoptosis of myocardial tissue in HF rats by promoting the expression of sirt1, thereby alleviating HF-induced myocardial injury.

**Key Words:**

Kallistatin, Heart failure, Inflammation, Apoptosis, Sirt1.

## Introduction

Heart failure (HF), as the end stage of most cardiovascular diseases, has extremely high morbidity and mortality<sup>1</sup>. More than 26 million people worldwide suffer from HF. In developed countries, the incidence of HF exceeds 1.5%<sup>2</sup>. The prognosis of HF is poor, and the 5-year survival rate is similar to common malignant tumors such as breast cancer and colorectal cancer<sup>3</sup>. The pathophysiological mechanism of HF is complex, including the activation of the renin-angiotensin-aldosterone system (RAAS) system, the excessive activation of sympathetic nerves and inflammatory factors, and myocardial cell apoptosis. Drug therapy (such as RAAS inhibitors,  $\beta$ -blockers, valsartan sodium, ivabradine, tolvaptan, etc.) has achieved certain progress and good clinical results<sup>4</sup>. But until now the pathogenesis of HF has not been fully understood. The medical treatment of HF still needs further improvement. Myocardial cell injury and loss caused by activation of the inflammatory system and myocardial cell apoptosis are the key factors for aggravating HF, and inhibition of ventricular remodeling caused by myocardial cell inflammation and apoptosis can improve the prognosis of HF, providing an effective approach for the prevention and treatment of HF<sup>5</sup>.

Kallistatin (KS) is a serine protease inhibitor, first isolated by Chao et al<sup>6</sup> from serum-free medium of human serum and human lung fibroblasts. KS plays an anti-inflammatory, anti-oxidative stress, and anti-apoptosis biological role in diseases such as sepsis, hypertension, tumors, and diabetic retinopathy<sup>7</sup>. In an animal study, recombinant human KS was injected into the tail vein of rats with sepsis, and it was found that KS could significantly reduce the inflammatory

response and organ damage caused by sepsis<sup>8</sup>. In addition, KS can inhibit tumor necrosis factor (TNF)- $\alpha$ -induced oxidative stress and apoptosis by activating phosphatidylinositol-3 kinase-serine threonine kinase-endothelial nitric oxide synthase (PI3K-Akt-eNOS) pathway<sup>9</sup>. However, the effect of KS on myocardial cell injury in HF has not been explored.

Therefore, in this study, we used doxorubicin to induce HF model in rats and used KS to treat HF rats to detect changes in the structure and function, inflammation and apoptosis of rat myocardial cells. In addition, we cultured rat myocardial cell line, H9c2 cells, to further verify the effect of KS on myocardial cell viability and apoptosis. We hope to provide new targets for clinical treatment of HF through this study.

## Materials and Methods

### Animals

40 healthy 8-week-old male Sprague Dawley (SD) rats were purchased from Anhui Medical University Experimental Animal Center. SD rats are housed in specific pathogen free (SPF)-class barrier facilities with room temperature of 22–26°C and relative humidity of 40–65%. The animal experiments in this study were approved by the Anhui Medical University Animal Experiment Ethics Committee.

### HF Model and Grouping

Rats were divided into control, HF, HF + low-dose KS (LKS) and HF + high-dose KS (HKS) groups. Doxorubicin was used to induce HF in rats of HF, HF + LKS and HF + HKS groups. After weighing the rats, we injected doxorubicin into rats intraperitoneally according to the dose of 2.5 mg/kg once a week for 6 weeks. The rats in the HF + LKS and HF + HKS groups were injected intraperitoneally with 1 mg/kg and 2 mg/kg of recombinant human KS (Abcam, Cambridge, MA, USA) daily from the first day of modeling<sup>10</sup>. Rats in the HF group were injected with an equal amount of normal saline intraperitoneally every day.

### Ultrasonic Cardiogram

One week after the last doxorubicin injection, we performed cardiac ultrasound (Visual Sonics, Toronto, Ontario, Canada) on all rats. First, we anesthetized the rat with 2% isoflu-

rane, then, we fixed the rat in a supine position on a constant temperature heating plate and fixed the limbs of the rat on four metal pole pieces. We placed the probe on the left margin of the rat sternum, and then, recorded the left ventricular end-diastolic diameter (LVEDd), left ventricular posterior wall depth (LVPWd) and left ventricular ejection fraction (LVEF) in M-mode ultrasound mode, and calculated the fractional shortening (FS).

### Enzyme Linked Immunosorbent Assay (ELISA)

ELISA was used to detect the concentration of brain natriuretic polypeptide (BNP) and inflammatory factors (interleukin (IL)-1 $\beta$ , IL-6, IL-8 and TNF- $\alpha$ ) (R&D Systems, Emeryville, CA, USA) in rat serum. We collected blood through the rat's subclavian vein. After leaving the blood at room temperature for 2 hours, we put it in a centrifuge (3000 rpm, 5 min, 4°C) and collected the supernatant (serum). Serum was stored in the refrigerator at -80°C. We use the standards in the ELISA kit to make a standard curve. Then, we calculated the concentration of BNP and inflammatory factors based on the absorbance of the sample and the standard curve.

### Histology and Hematoxylin-Eosin (HE) Staining

After collecting the rat heart, we washed the heart with normal saline and fixed it with 4% paraformaldehyde for 24 hours. Then, we put the heart tissue in gradient alcohol, xylene and paraffin in turn to make paraffin blocks. Then, we use a microtome (LEICA RM2235, Koln, Germany) to make paraffin sections. Paraffin sections were placed in a 37°C incubator for 3 days and kept at room temperature for long-term storage.

We first put the paraffin sections in a 65°C incubator for 1 hour. Then, we put the sections in xylene and gradient alcohol for dewaxing and hydration. After washing the sections with running water, we stained the cell nucleus with hematoxylin solution (Sigma-Aldrich, St. Louis, MO, USA). 1% hydrochloric acid alcohol was used to differentiate the excess hematoxylin stain. Then, we put the sections in the eosin solution (Sigma-Aldrich, St. Louis, MO, USA) for 1 minute and continue to put them in alcohol and xylene. Finally, we use neutral gum to seal the sections and observe the staining results using an optical microscope (LEICA, Koln, Germany).

### Immunohistochemical (IHC) Staining

After baking the sections in a 65°C incubator for 1 hour, we placed the sections in xylene and gradient alcohol for dewaxing and hydration. Then, we put the sections into the antigen repair box and added ethylene diamine tetraacetic acid antigen repair solution. The antigen repair kit was placed in a microwave oven and heated for 15 minutes. Then, we took out the antigen repair kit and left it to cool naturally at room temperature. We washed the sections with phosphate-buffered saline (PBS) and blocked endogenous peroxidase with 3% H<sub>2</sub>O<sub>2</sub>. After washing the sections with PBS, we blocked myocardial tissue with 10% goat serum for 30 minutes. Then, we used primary antibody dilution (sirt1, ab110304; caspase3, ab13847; caspase9, ab202068; Abcam, Cambridge, MA, USA) to incubate myocardial tissue overnight at 4°C. After washing the sections with PBS, we used secondary antibody dilution (GeneTech, Shanghai, China) to incubate myocardial tissue at room temperature for 2 hours. Then, we used diaminobenzidine (DAB; GeneTech, Shanghai, China) for color development and hematoxylin staining for cell nucleus. Finally, we use an optical microscope (LEICA, Koln, Germany) to observe the staining results.

### Cell Culture

Rat myocardial cell line (H9c2 cells) was used in this study. Dulbecco's Modified Eagle's Medium (DMEM; Gibco, Rockville, MD, USA) containing 10% fetal bovine serum (FBS; Gibco, Rockville, MD, USA) and 1% double antibody (Gibco, Rockville, MD, USA) was used to culture H9c2 cells. Cells were cultured in a 37°C incubator with 5% CO<sub>2</sub>. 400 µM H<sub>2</sub>O<sub>2</sub> was used to induce H9c2 cell injury.

### RNA Isolation and Quantitative Reverse Transcription-Polymerase Chain Reaction (qRT-PCR)

We used the TRIzol (Sigma-Aldrich, St. Louis, MO, USA) method to extract total RNA from myocardial tissue and H9c2 cells. A spectrophotometer (LASPEC, Shanghai, China) was used to detect RNA concentration. HiScript II Q RT SuperMix (Vazyme, Nanjing, China) is used to reverse mRNA to complementary deoxyribose nucleic acid (cDNA). The reverse transcription system is 1 µg template RNA + 4 µL HiScript II Q RT SuperMix + RNase-free ddH<sub>2</sub>O to 20 µL. The reaction time was 50°C for 15 minutes and 85°C for 5 seconds. The cDNA obtained by reverse transcription was stored in a refrigerator at -20°C. Then, we used SYBR Green Master Mix (Vazyme, Nanjing, China) and corresponding primers to amplify cDNA. Glyceraldehyde 3-phosphate dehydrogenase (GAPDH) expression was used as control. 2<sup>-ΔΔCt</sup> was used to represent the relative expression of mRNA. Primer sequences were shown in Table I.

### Cell Transfection

SiRNA-negative control (NC) and siRNA-sirt1 were used to transfect H9c2 cells. We seeded H9c2 cells in 6-well plates. After the cell fusion reached 50%, we used Lipofectamine 3000 reagent (Invitrogen, Carlsbad, CA, USA) to transfect siRNA-NC and siRNA-sirt1 into H9c2 cells. RT-PCR was used to detect transfection efficiency.

### Immunofluorescent (IF) Staining

We seeded H9c2 cells in 6-well plates. After stimulating H9c2 cells with H<sub>2</sub>O<sub>2</sub> and KS, we discarded the medium in the 6-well plate and fixed

Table I. RT-PCR primer sequences.

Name	Sense/Anti-sense	Sequences (5'-3')
sirt1	Sense	GAGTGTGCTGGAGGATCTG
	Anti-sense	TGCTCTGATTTGTCTGGTGT
caspase3	Sense	TCCACGAGCAGAGTCAAA
	Anti-sense	GCCAACCAAGTTCACACA
caspase9	Sense	CCTGTATCATCCCCACCCT
	Anti-sense	GCCGAGACCTTGGAACAC
Bcl2	Sense	GGGGAACACACAGAATCA
	Anti-sense	GGCCCGAAAGAGAGAAA
Bax	Sense	CAGGATCGAGCAGAGAGGA
	Anti-sense	TGTCCAGTTCATCGCCAA
GAPDH	Sense	TCTTTGCTTGGGTGGGT
	Anti-sense	TGGGTCTGGCATTGTTCT

the cells with 4% paraformaldehyde for 15 minutes. After washing the cells with PBS, we treated the cells with 0.1% Triton X-100 for 20 minutes. Then, we used 10% goat serum to incubate the cells for 1 hour. After discarding goat serum, we used primary antibody dilution (caspase3, ab13847, Abcam, Cambridge, MA, USA) to incubate the cells at 4°C overnight. After washing the cells with PBS, we used fluorescent secondary antibody dilution to incubate the cells in the dark for 1 hour and washed the cells with PBS again. DAPI was used to stain the cell nucleus. Finally, we use a fluorescence microscope (LEICA, Koln, Germany) to observe the staining results.

### **Cell Counting Kit-8 (CCK8) Assay**

We seeded H9c2 cells in 96-well plates with approximately 5000 cells per well. After stimulating H9c2 cells with H<sub>2</sub>O<sub>2</sub> and KS, we added 10 µL of CCK8 reagent (Dojindo Molecular Technologies, Kumamoto, Japan) to each well. After putting the 96-well plate in the incubator for 2 hours, we took out the 96-well plate and used a microplate reader to detect the absorbance (OD) of each well at 450nm wavelength. Blank wells had only the culture medium and no cells; the control wells had cells but were not treated. Cell viability =  $(OD_{\text{sample}} - OD_{\text{blank}}) / (OD_{\text{control}} - OD_{\text{blank}})$ .

### **Statistical Analysis**

Statistical Product and Service Solutions (SPSS) 21.0 statistical software (IBM Corp., Armonk, NY, USA) was used to analyze the data of this study. All measurement data are expressed as mean ± standard deviation. Differences between two groups were analyzed by using the Student's *t*-test. Comparison between multiple groups was done using One-way ANOVA test followed by Post-Hoc Test (Least Significant Difference). *p* < 0.05 indicated that the difference was statistically significant. All experiments were repeated 3 times.

## **Results**

### **KS Relieved Doxorubicin-Induced Rat HF**

To clarify the effect of KS on rat HF, we used doxorubicin to induce rat HF and treated rats with 1 mg/kg and 2 mg/kg recombinant human KS. After 6 weeks, we measured the heart weight (HW) (Figure 1A) and body weight (BW) (Figure 1B) of the rats. Compared with the rats in the control group, the BW of the rats in the HF

group decreased while the HW increased. After the rats were treated with KS, the BW of the rats increased and the HW decreased. Therefore, doxorubicin increased HW/BW in rats, while KS inhibited the effect of doxorubicin (Figure 1C). The concentration of BNP in rat serum was found to be significantly higher than the control group, while KS effectively reduced the concentration of BNP (Figure 1D). The results of echocardiography showed that the LVEF (Figure 1E), FS (Figure 1F) and LVPWd (Figure 1G) of HF rats were lower than that of the control group, while the LVEDd (Figure 1H) of HF rats were higher than the control group. After treatment with KS, the cardiac function of the rats was significantly improved. HE staining found that the myocardial tissue of the HF group was disordered and the number of myocardial cells decreased, while the myocardial structure of the HF + LKS and HF + HKS group was significantly improved (Figure 1I). IHC detected the expression of sirt1 in rat myocardium. The expression of sirt1 in myocardial tissue of HF rats decreased, while KS increased the expression of sirt1 in myocardial tissue of rats (Figure 1J). The above results indicated that KS effectively alleviated doxorubicin-induced HF, but there was no significant difference between the rats in the HF + LKS and HF + HKS groups.

### **KS Reduced Inflammation in HF Rats**

To determine the effect of KS on inflammation in HF rats, we detected the expression of inflammatory factors in rat serum and myocardial tissue. ELISA detected the concentration of IL-1β (Figure 2A), IL-6 (Figure 2B), IL-8 (Figure 2C) and TNF-α (Figure 2D) in rat serum. After using doxorubicin to induce rat HF, the expression of inflammatory factors in rat serum increased significantly, indicating that rat HF was accompanied by an increase in inflammation level. The treatment of KS significantly reduced the concentration of inflammatory factors in rat serum. The results of RT-PCR also showed that KS reduced the inflammation level of myocardial tissue in HF rats (Figure 2E-H).

### **KS Reduced Myocardial Cell Apoptosis in HF Rats**

HF is accompanied by a decrease in apoptosis and number of myocardial cells, so we detected the effect of KS on the rat myocardial cell apoptosis. IHC staining detected the expression of caspase3 and caspase9 in rat myo-



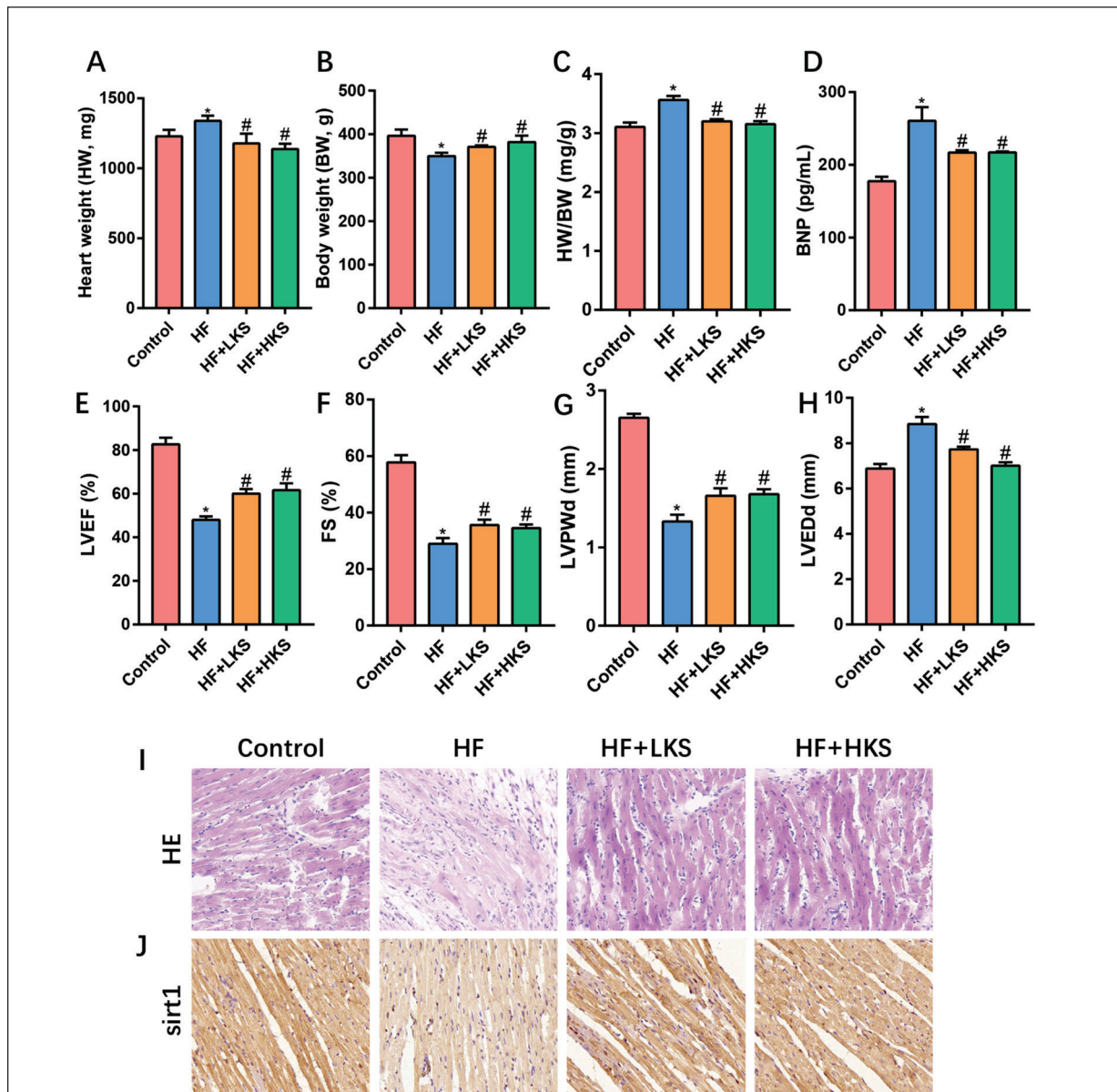


**Figure 1.** KS relieved doxorubicin-induced rat HF. **A-C**, HW, BW and HW/BW in rats of four groups. **D**, Concentration of BNP in rat serum of four groups. **E-H**, The cardiac function of rats was detected by ultrasonic cardiogram. **I**, HE staining of rat myocardium in four groups (magnification: 200×). **J**, Expression of sirt1 in rat myocardium was determined by IHC staining (magnification: 200×). (“\*” means  $p < 0.05$  vs. control group; “#” means  $p < 0.05$  vs. HF group).

cardium (Figure 3A). The induction of doxorubicin increased the expression of caspase3 and caspase9, while the KS inhibited the expression of these apoptosis-related molecules. RT-PCR detected the expression of caspase3 (Figure 3B), caspase9 (Figure 3C), Bcl2 (Figure 3D) and Bax (Figure 3E). KS was found to reduce the mRNA expression of caspase3, caspase9 and Bax and increase the mRNA expression of the anti-apoptotic molecule Bcl2.

#### ***Inhibition of Sirt1 Reduced the Protective Effect of KS on H9c2 Cells***

To determine whether sirt1 mediated the protective effect of KS on myocardial cells, we used KS and siRNA-sirt1 to treat H9c2 cells. The CCK8 assay examined the effect of 10 nM, 50 nM, 100 nM, 200 nM and 500 nM of KS on the viability of H9c2 cells (Figure 4A). 100 nM was found to be the optimal concentration of KS to stimulate H9c2 cells, so we used 100 nM KS to stimulate

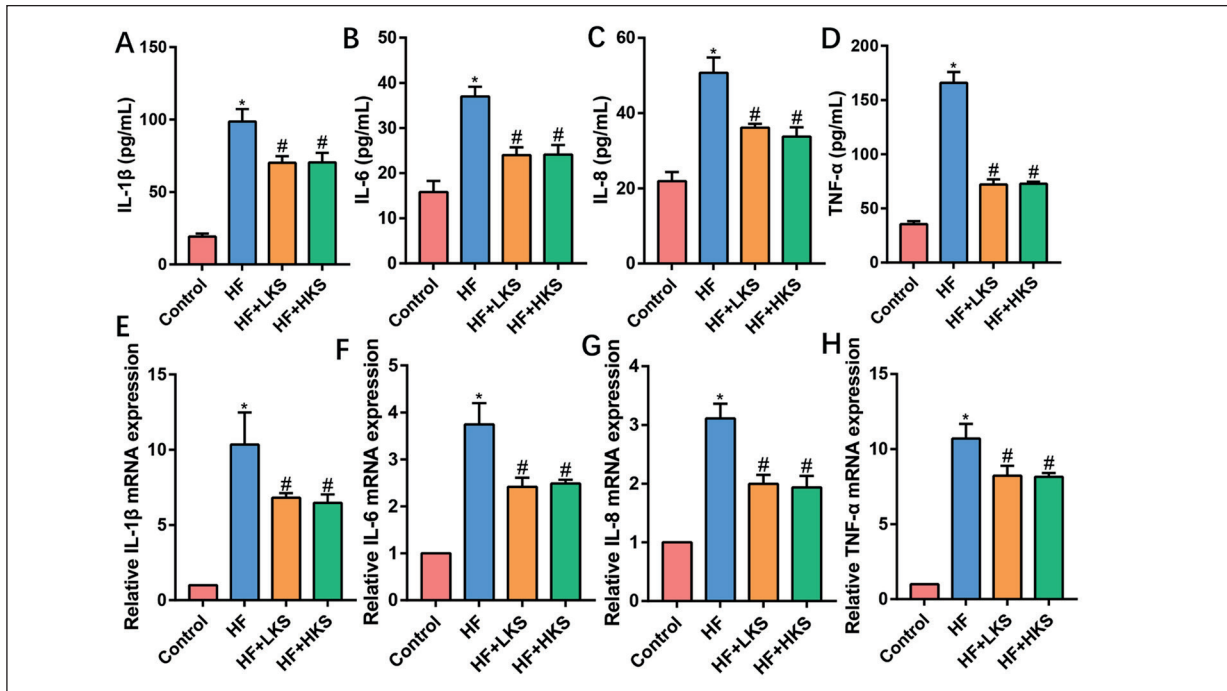


**Figure 2.** KS reduced inflammation in HF rats. **A-D**, concentration of IL-1β, IL-6, IL-8 and TNF-α in rat serum of four groups was determined by ELISA. **E-H**, mRNA expression of IL-1β, IL-6, IL-8 and TNF-α in rat myocardium of four groups was determined by RT-PCR. (“\*” means  $p < 0.05$  vs. control group; “#” means  $p < 0.05$  vs. HF group).

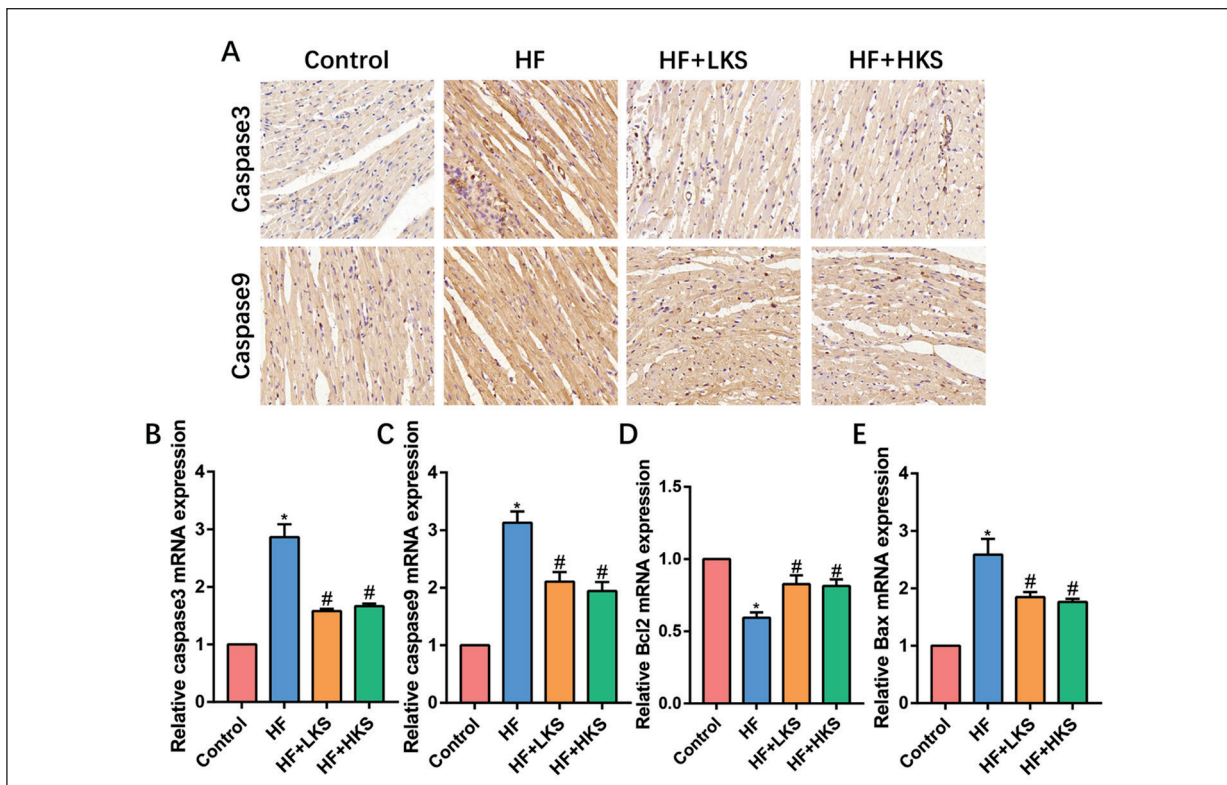


**Figure 3.** KS reduced myocardial cell apoptosis in HF rats. **A**, expression of caspase3 and caspase9 in rat myocardium was determined by IHC staining (magnification: 200×). **B-E**, mRNA expression of caspase3, caspase9, Bcl2 and Bax in rat myocardium was determined by RT-PCR. (“\*” means  $p < 0.05$  vs. control group; “#” means  $p < 0.05$  vs. HF group).

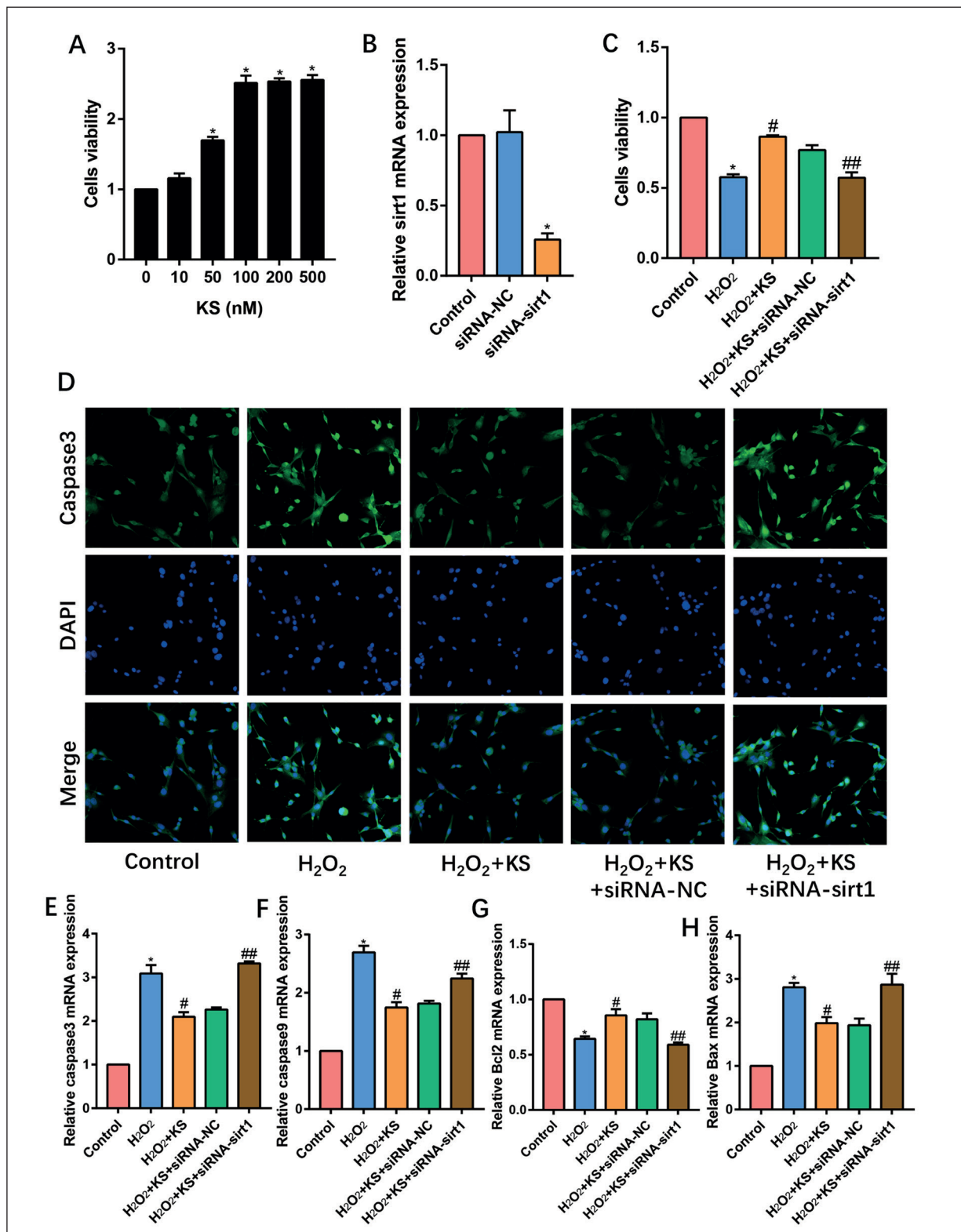


**Figure 4.** Inhibition of sirt1 reduced the protective effect of KS on H9c2 cells. **A**, CCK-8 assay determined the optimum concentration of KS to stimulate H9c2 cells. **B**, mRNA expression of sirt1 in H9c2 cells transfected with siRNA-NC and siRNA-sirt1. **C**, cell viability of H9c2 cells was determined by CCK8 assay. **D**, IF staining detected the caspase3 in H9c2 cells (magnification: 200×). **E-H**, mRNA expression of caspase3, caspase9, Bcl2 and Bax in H9c2 cells. (“\*” means  $p < 0.05$  vs. control group; “#” means  $p < 0.05$  vs. H<sub>2</sub>O<sub>2</sub> group; “##” means  $p < 0.05$  vs. H<sub>2</sub>O<sub>2</sub>+KS+siRNA-NC group).

H9c2 cells in subsequent experiments. RT-PCR detected the transfection efficiency of siRNA-sirt1 and found that siRNA-sirt1 effectively suppressed the expression of sirt1 in H9c2 cells (Figure 4B). The cells were divided into control,  $H_2O_2$ ,  $H_2O_2$  + KS,  $H_2O_2$  + KS + siRNA-NC and  $H_2O_2$  + KS + siRNA-sirt1 groups. CCK8 assay detected the proliferation ability of cells in each group (Figure 4C). After suppressing the expression of sirt1, the promotion effect of KS on H9c2 cells viability decreased. IF staining found that the inhibition of sirt1 reduced the inhibitory effect of KS on caspase3 (Figure 4D). Results of RT-PCR also showed that the inhibition of sirt1 attenuated the anti-apoptotic effect of KS (Figure 4E-4H).

## Discussion

HF is the end result of various cardiovascular diseases. The most common causes include coronary heart disease, hypertension, cardiomyopathy, and valvular heart disease. Its morbidity and mortality are increasing year by year, posing a serious threat to human health<sup>11</sup>. Our study found that KS had a good therapeutic effect on doxorubicin-induced rat HF model. By reducing the level of inflammation in rat circulation and myocardial tissue, and the level of rat myocardial cell apoptosis, KS effectively improved the structure and function of myocardium in HF rats. In the H9c2 cell injury induced by  $H_2O_2$ , KS improved the viability of H9c2 cells and reduced the level of apoptosis. These results indicated that KS may have a potential therapeutic effect on HF-induced myocardial injury.

BNP is a cardiac circulating hormone that maintains homeostasis by regulating the functions of the heart, vascular smooth muscle, and kidneys. BNP is an important marker of HF<sup>12</sup>. After cardiomyocytes are stimulated, BNP gene expression will increase. The concentration of BNP and N-Terminal Pro-form BNP (NT-pro BNP) is significantly positively correlated with cardiac function grading, which is an effective means of diagnosing HF. NT-pro BNP > 5000 ng/L means that the recent mortality of HF is high; NT-pro BNP > 1000 ng/L means that the long-term mortality of HF is high<sup>13</sup>. Therefore, Kallistatin lowering BNP meant that KS can protect cardiomyocytes.

In HF, inflammatory cytokines participate in regulating left ventricular function and play an important role in myocardial remodeling<sup>14</sup>.

Melendez et al<sup>15</sup> found that injecting IL-6 into rats resulted in left ventricular myocardial hypertrophy, increased ventricular muscle stiffness, increased collagen volume fraction, and a proportional increase in myocardial cell width and length<sup>15</sup>. Hamid et al<sup>16</sup> showed that continuous activation of NF- $\kappa$ B p65 can accelerate ventricular remodeling through pro-inflammatory, pro-fibrotic and pro-apoptotic mechanisms. KS has been found to have anti-inflammatory effects in various diseases. Yin et al<sup>17</sup> detected that KS can fight vasculitis through various biological effects, thereby delaying the progress of the disease. In addition, Zhou et al<sup>18</sup> on renal ischemia-reperfusion injury (IRI) revealed that KS gene-transfected IRI mice showed reduced renal injury and reduced tubular necrosis and apoptosis. Therefore, we detected the expression changes of IL-1 $\beta$ , IL-6, IL-8 and TNF- $\alpha$  in the myocardium of HF rats. The inflammatory factors in the serum and inflammatory factor mRNA in myocardial tissue of HF rats treated with KS were significantly reduced, indicating that KS had a significant anti-inflammatory effect on the myocardial tissue of HF rats.

Primary myocardial injury (such as myocardial infarction and cardiomyopathy, etc.) and increased load (including volume and pressure load) cause a large number of myocardial cell apoptosis, resulting in a gradual decline in cardiac function<sup>19</sup>. Yang et al<sup>20</sup> demonstrated that HF was accompanied by a decrease in the expression of anti-apoptotic molecule Bcl2 in myocardial cells, and microRNA-19b-1 can alleviate myocardial apoptosis caused by HF by targeting Bcl2. Yao et al<sup>21</sup> also found that a new type of non-canonical pathway can inhibit the myocardial cell apoptosis in HF by regulating endoplasmic reticulum stress. In our study, we detected the effect of KS on the myocardial cell apoptosis by detecting the key molecule caspase3/9 in the caspase family and Bcl2/Bax in the Bcl family. The decrease of caspase3/9 and Bax and the increase of Bcl2 by KS indicated its inhibition of myocardial cell apoptosis. This again proved the protective effect of KS on myocardial cells.

Sirt1 is a deacetylase that depends on nicotinamide adenosine dinucleotide (NAD<sup>+</sup>) through its deacetylation activity in mammals<sup>22</sup>, and thus participates in various biological processes such as DNA damage repair, gene transcription regulation, cell apoptosis, metabolism and aging. Yu et al<sup>23</sup> have shown that sirt1 can reduce the inflammation caused by myocardial hypertrophy,



smoking, and HF<sup>24</sup>. After sirt1 gene knockout, the expression of related inflammatory factors in mice, such as IL-1 $\beta$  and TNF- $\alpha$ , increased significantly, and sirt1 reduced the endothelial cells injury by reducing stress, thereby inhibiting the inflammatory response<sup>25</sup>. In addition, sirt1 can deacetylate many nuclear transcription factors, such as p53, Ku70, and FOXO, thereby preventing downstream apoptotic reactions<sup>26</sup>. Dell’Omo et al<sup>27</sup> has shown that sirt1 can inhibit high phosphorus-induced vascular calcification. The mechanism is related to sirt1 regulating p53/p21 pathway activity and inhibiting apoptosis. We found that KS promoted the expression of sirt1 in myocardial cells, and the inhibition of sirt1 in H9c2 cells weakened the protective effect of KS on myocardial cells. This indicated that sirt1 mediated the myocardial protection of KS, and this also explained the anti-inflammatory and anti-apoptotic effects of KS on the myocardial tissue of HF rats. Therefore, KS has potential application prospects for the treatment of HF.

To sum up, KS showed good therapeutic potential for HF. This is the first study to investigate the effect of KS on HF. We hoped that this study would provide a new breakthrough in improving the prognosis of HF patients clinically.

## Conclusions

The above results revealed that HF is accompanied by increased levels of inflammation and apoptosis. Our study was the first to found that KS reduced the inflammation and apoptosis of myocardial tissue by promoting the expression of sirt1, thereby relieving HF-induced myocardial injury.

## Conflict of Interest

The Authors declare that they have no conflict of interests.

## References

- DI PALO KE, BARONE NJ. Hypertension and heart failure: prevention, targets, and treatment. *Heart Fail Clin* 2020; 16: 99-106.
- SLIVNICK J, LAMPERT BC. Hypertension and heart failure. *Heart Fail Clin* 2019; 15: 531-541.
- PFEFFER MA, SHAH AM, BORLAUG BA. Heart failure with preserved ejection fraction in perspective. *Circ Res* 2019; 124: 1598-1617.
- VADUGANATHAN M, JANUZZI JJ. Preventing and treating heart failure with sodium-glucose co-transporter 2 inhibitors. *Am J Cardiol* 2019; 124 Suppl 1: S20-S27.
- JIA Q, LI H, ZHOU H, ZHANG X, ZHANG A, XIE Y, LI Y, LV S, ZHANG J. Role and effective therapeutic target of gut microbiota in heart failure. *Cardiovasc Ther* 2019; 2019: 5164298.
- CHAO J, MIAO RQ, CHEN V, CHEN LM, CHAO L. Novel roles of kallistatin, a specific tissue kallikrein inhibitor, in vascular remodeling. *Biol Chem* 2001; 382: 15-21.
- CHAO J, LI P, CHAO L. Kallistatin: double-edged role in angiogenesis, apoptosis and oxidative stress. *Biol Chem* 2017; 398: 1309-1317.
- LI P, GUO Y, BLEDSOE G, YANG ZR, FAN H, CHAO L, CHAO J. Kallistatin treatment attenuates lethality and organ injury in mouse models of established sepsis. *Crit Care* 2015; 19: 200.
- SHEN B, GAO L, HSU YT, BLEDSOE G, HAGIWARA M, CHAO L, CHAO J. Kallistatin attenuates endothelial apoptosis through inhibition of oxidative stress and activation of Akt-eNOS signaling. *Am J Physiol Heart Circ Physiol* 2010; 299: H1419-H1427.
- HUANG X, WANG X, LV Y, XU L, LIN J, DIAO Y. Protection effect of kallistatin on carbon tetrachloride-induced liver fibrosis in rats via antioxidative stress. *PLoS One* 2014; 9: e88498.
- MILICIC D, JAKUS N, FABIJANOVIC D. Microcirculation and heart failure. *Curr Pharm Des* 2018; 24: 2954-2959.
- HARRISON TG, SHUKALEK CB, HEMMELGARN BR, ZARNKE KB, RONKSLEY PE, IRAGORRI N, GRAHAM MM AND JAMES MT. Association of NT-proBNP and BNP with future clinical outcomes in patients with ESKD: A systematic review and meta-analysis. *Am J Kidney Dis* 2020; S0272-6386(20)30530-8. doi: 10.1053/j.ajkd.2019.12.017. Online ahead of print.
- RODRÍGUEZ-CASTRO E, HERVELLA P, LÓPEZ-DEQUIDT I, ARIAS-RIVAS S, SANTAMARÍA-CADAVID M, LÓPEZ-LOUREIRO I, DA SILVA-CANDAL A, PÉREZ-MATO M, SOBRINO T, CAMPOS F, CASTILLO J, RODRÍGUEZ-YÁÑEZ, IGLESÍAS-REY R. NT-pro-BNP: a novel predictor of stroke risk after transient ischemic attack. *Int J Cardiol* 2020; 298: 93-97.
- SHIRAZI LF, BISSETT J, ROMEO F, MEHTA JL. Role of inflammation in heart failure. *Curr Atheroscler Rep* 2017; 19: 27.
- MELENDEZ GC, McLARTY JL, LEVICK SP, DU Y, JANICKI JS, BROWER GL. Interleukin 6 mediates myocardial fibrosis, concentric hypertrophy, and diastolic dysfunction in rats. *Hypertension* 2010; 56: 225-231.
- HAMID T, GUO SZ, KINGERY JR, XIANG X, DAWN B, PRABHU SD. Cardiomyocyte NF-kappaB p65 promotes adverse remodelling, apoptosis, and endoplasmic reticulum stress in heart failure. *Cardiovasc Res* 2011; 89: 129-138.
- YIN H, GAO L, SHEN B, CHAO L, CHAO J. Kallistatin inhibits vascular inflammation by antagonizing tumor necrosis factor-alpha-induced nuclear factor kappaB activation. *Hypertension* 2010; 56: 260-267.

- 18) ZHOU S, SUN Y, ZHUANG Y, ZHAO W, CHEN Y, JIANG B, GUO C, ZHANG Z, PENG H, CHEN Y. Effects of kallistatin on oxidative stress and inflammation on renal ischemia-reperfusion injury in mice. *Curr Vasc Pharmacol* 2015; 13: 265-273.
- 19) JOSE CJ, VATNER DE, VATNER SF. Myocardial apoptosis in heart disease: does the emperor have clothes? *Basic Res Cardiol* 2016; 111: 31.
- 20) YANG W, HAN Y, YANG C, CHEN Y, ZHAO W, SU X, YANG K, JIN W. MicroRNA-19b-1 reverses ischaemia-induced heart failure by inhibiting cardiomyocyte apoptosis and targeting Bcl2 l11/BIM. *Heart Vessels* 2019; 34: 1221-1229.
- 21) YAO Y, LU Q, HU Z, YU Y, CHEN Q, WANG QK. A non-canonical pathway regulates ER stress signaling and blocks ER stress-induced apoptosis and heart failure. *Nat Commun* 2017; 8: 133.
- 22) ALVES-FERNANDES DK, JASIULIONIS MG. The role of SIRT1 on DNA damage response and epigenetic alterations in cancer. *Int J Mol Sci* 2019; 20: 3153.
- 23) YU Q, DONG L, LI Y, LIU G. SIRT1 and HIF1alpha signaling in metabolism and immune responses. *Cancer Lett* 2018; 418: 20-26.
- 24) YAN T, HUANG J, NISAR MF, WAN C, HUANG W. The beneficial roles of SIRT1 in drug-induced liver injury. *Oxid Med Cell Longev* 2019; 2019: 8506195.
- 25) CAO M, ZHANG W, LI J, ZHANG J, LI L, LIU M, YIN W, BAI X. Inhibition of SIRT1 by microRNA-9, the key point in process of LPS-induced severe inflammation. *Arch Biochem Biophys* 2019; 666: 148-155.
- 26) FUJITA Y, YAMASHITA T. Sirtuins in neuroendocrine regulation and neurological diseases. *Front Neurosci* 2018; 12: 778.
- 27) DELL'OMO G, CRESCENTI D, VANTAGGIATO C, PARRAVICINI C, BORRONI AP, RIZZI N, GAROFALO M, PINTO A, RECORDATI C, SCANZIANI E, BASSI FD, PRUNERI G, CONTI P, EBERINI I, MAGGI A, CIANA P. Inhibition of SIRT1 deacetylase and p53 activation uncouples the anti-inflammatory and chemopreventive actions of NSAIDs. *Br J Cancer* 2019; 120: 537-546.